

# Molecular Dynamics Simulation of Reduction of the Surface Layer Porosity in a BCC Crystal Induced by Laser Pulses

A. V. Markidonov<sup>a,c,\*</sup> (ORCID: 0000-0002-4566-528X)<sup>†</sup>,  
M. D. Starostenkov<sup>b,\*\*</sup> (ORCID: 0000-0002-6326-7613),  
A. N. Gostevskaya<sup>c,\*\*\*</sup> (ORCID: 0000-0002-7328-5444),  
D. A. Lubyanyoy<sup>d,\*\*\*\*</sup> (ORCID: 0000-0001-9773-3558),  
and P. V. Zakharov<sup>e,\*\*\*\*\*</sup> (ORCID: 0000-0002-6410-1594)

<sup>a</sup> Kuzbass Humanitarian Pedagogical Institute, Kemerovo State University, Novokuznetsk, 654041 Russia

<sup>b</sup> Altai State Technical University, Barnaul, 656038 Russia

<sup>c</sup> Siberian State Industrial University, Novokuznetsk, 654006 Russia

<sup>d</sup> Gorbachev Kuzbass State Technical University, Prokopyevsk Branch, Prokopyevsk, 653039 Russia

<sup>e</sup> Peter the Great St. Petersburg Polytechnic University, St. Petersburg, 195251 Russia

\*e-mail: markidonov\_artem@mail.ru

\*\*e-mail: genphys@mail.ru

\*\*\*e-mail: lokon1296@mail.ru

\*\*\*\*e-mail: lubjanoy@yandex.ru

\*\*\*\*\*e-mail: zakharovpvl@rambler.ru

Received May 3, 2023; revised May 17, 2023; accepted May 29, 2023

**Abstract**—A deeper understanding of the interaction of laser radiation with matter can facilitate the development of technologies for laser synthesis of materials with unique properties, nanostructuring of surfaces of processed solids, etc. The difficulties related to direct observations of various fast processes contribute to the progress in the computer simulation methods used to study them. This work presents the results of the simulation of reduction of the iron surface layer porosity induced by laser pulses. The investigations have been carried out using the potential calculated within the embedded atom method. The model under study has been subjected to structural analysis using the proven algorithms, which makes it possible to quantify the surface area of pores in the bulk of a crystal. The computational cells under consideration contain pores in the amorphous region, which remain stable upon the model cooling corresponding to the natural cooling of a solid in the environment described by a mathematical expression. Obviously, to get rid of defects, a solid should be annealed. It is shown that, after annealing at a temperature of no higher than half of the melting point, pores are preserved. Taking into account that the main mechanisms for reducing the porosity are the diffusion-viscous flow of matter into pores and that diffusion in the amorphous phase is more intense than in the crystalline one, the conditions for slowing down crystallization at a certain temperature should be established in the model. The required conditions have been achieved by straining the computational cell. It is shown that, as a result, the number of pores decreases under both compression and tension.

**Keywords:** model, temperature, pore, crystallization, strain

**DOI:** 10.1134/S1063783423700038

## INTRODUCTION

Nanosecond laser pulses are widely used in materials processing. The interaction of laser radiation with the surface of a solid body is a fairly complex process, which represents a combination of several physical phenomena. Surface heating under such an impact leads to laser-induced phase transitions, the kinetics of which differs from that of similar processes upon slower heating [1]. In addition, various defect forma-

tions occur in the surface layers of a material: ablation craters, dislocation and crack clusters, pores, etc. [2–6]. Obviously, a more detailed study of the defect formation and subsequent evolution of the defect structure is an urgent task, since laser technologies for materials processing have a number of advantages. However, the main difficulties lie in the impossibility of direct observations of such fast processes. Therefore, in this case, computer simulation can be considered as one of the priority examination methods.

<sup>†</sup> Deceased.

Previously, the authors used the molecular dynamics simulation to explore structural changes in the surface layers of a crystal under a high-energy external impact leading to nonuniform heating followed by natural cooling [8, 9]. Visualization of a computational cell subjected to such an impact disclosed the formation of pores in the amorphous region, which were gradually filled with a substance. At the same time, the laser radiation energy densities were identified at which the pores formed remain unfilled throughout the entire simulation time. It is interesting to establish the conditions that would make it possible to get rid of these pores, which is what this study was aimed at.

## EXPERIMENTAL

The molecular dynamics method was chosen for the investigations, since it allows modeling of various statistical ensembles and comparing model time with physical time. The computational cell consisted of 48 000 particles and the interaction between them was described using a potential calculated by the embedded atom method, the parameters of which were borrowed from [10]. The characteristics of the model were selected in such a way that it corresponded to the  $\alpha$ -Fe crystal. To simulate the infiniteness of the crystal along the  $X$  and  $Z$  coordinate axes, periodic boundary conditions were used and, to simulate the surface along the  $Y$  axis, free boundary conditions were used. The equations of motion were integrated using the Verlet velocity algorithm with a time step of 1 fs. Taking into account that a canonical ensemble was modeled, a constant temperature was maintained using a proportional thermostat. All computations were carried out in the freely distributed XMD package [11].

The simulation results obtained in [8, 9] were used as an initial particle configuration under study. Figure 1a shows the computation cell obtained after 30 ps of model time at a laser radiation energy density of 465 MW/cm<sup>2</sup>. The particles identified as having a local environment corresponding to the bcc crystal lattice are highlighted. The identification was carried out using the Ackland–Jones method of angles and bonds [12], which analyzes the distribution of angles formed by pairs of neighbors of the central atom. The nearest environment of colorless particles is not identified as having long-range order and is considered to belong to the amorphous phase. In addition, in Fig. 1a, one can see agglomerations of particles detached from the surface. In the further investigation, they are removed from the system and ignored.

Figure 1b presents a visualization of pores in the computational cell by the Edelsbrunner and Mücke alpha-form method, in which a geometric set of points is united by a surface mesh using Delaunay tetrahedrization followed by the smoothing procedure. In this method, a pore in the bulk is identified by inscribing a virtual sphere into the interparticle space. In the cal-

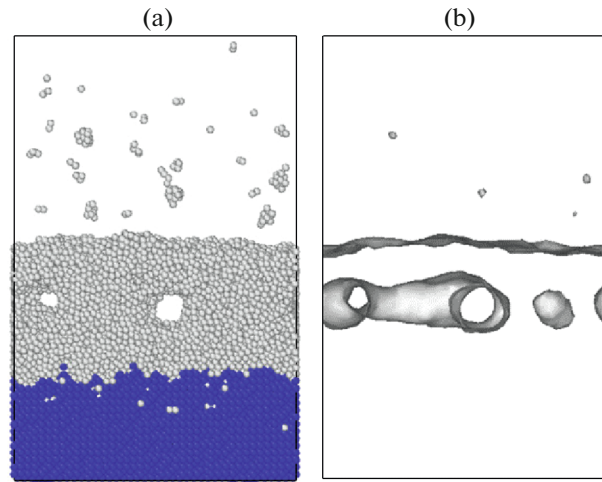


**Fig. 1.** Visualization of the initial configuration of (a) the computational cell and (b) pores contained in it.

ulation, the radius of the sphere was set equal to the interatomic spacing and, therefore, the failure of particles to fall into this sphere was considered as a pore.

The simulated computational cell was visualized using the OVITO package [13].

## RESULTS AND DISCUSSION

As reported previously, the investigated pore remains stable during the simulation of natural cooling, which is achieved by a gradual decrease in the temperature of the computational cell according to the established regularity. Therefore, at the initial stage, the computational cell was subjected to annealing at a constant temperature. To estimate changes in the size of pores after their gradual filling with matter, the surface of pores in the cell volume was calculated (with disregard of the crystal free surface) using the above-described Delaunay method. Obviously, a larger number of pores will be formed in a coarser computational cell, so the calculated surface areas were converted into dimensionless values, which are the ratio between the pore and computational cell surface areas. In addition, the annealing temperature specified during the simulation must be compared with some known value, for which the melting point of iron was chosen. The results of the calculation are shown in Fig. 2.

As follows from Fig. 2, at an annealing temperature below  $0.5T_{\text{melt}}$ , pores are preserved in the computation cell. Hence, one can get rid of pores directly by annealing only at relatively high temperatures. Previously [8, 9], the authors considered the diffusion-viscous flow of matter into pores as the main mechanism for removal of pores. Obviously, this process depends, to a great extent, on the temperature of the computation cell; therefore, at a low annealing temperature, pores are retained.

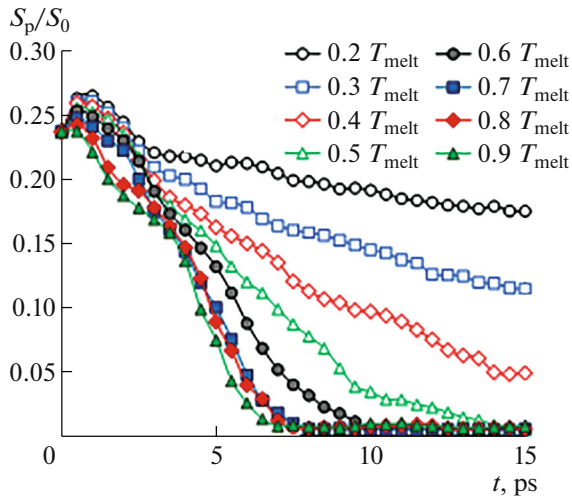


**Fig. 2.** Change in the relative free surface of pores in the computational cell ( $S_p$  is the pore surface area and  $S_0$  is the surface area of the computational cell at the initial instant of time) during the simulation while maintaining a constant temperature (given as a fraction of melting point  $T_{melt}$ ).

If we visualize the structural change upon annealing, we will notice that the crystallization front propagating during the simulation bends around pores without causing them to be completely filled with a substance (see Fig. 3) and the pores initially contained in the amorphous region remain after the crystallization. Taking into account that diffusion in an amorphous body proceeds more intensively than in a crystalline one, which can have different explanations [14, 15], in the crystalline region, a pore remains stable at a specified temperature.

The driving force of the crystallization is the trend of a system to achieve the state with the minimum free energy and the greater the difference in the free energies of the liquid and solid phases, the higher the speed of motion of the crystallization front. Therefore, a way to slow down the front can be to reduce this difference by increasing the free energy of the solid phase, for example, via straining the computation cell. Therefore, at the next stage of the study, the force impact on

the crystal was simulated. The strain was created by changing the equilibrium lattice parameter. The biaxial straining along the  $X$  and  $Z$  axes was considered. The pore surface areas calculated at different strains of the computation cell are presented in Fig. 4.

Under the compressive straining, pores decrease more intensively, since, in this case, in addition to a decrease in the speed of the crystallization front, the free volume in the lattice decreases and the surface area is reduced. Under the tensile straining, the pore volume increases; therefore, if the straining of the computational cell is small, the diffusion-viscous flow of matter into the pore cannot dominate with a decrease in the crystallization front speed, but under straining with a value of 5%, this mechanism starts prevailing and the pore surface area begins to rapidly decrease.

To confirm the reduction of the speed of the crystallization front under straining of the computational cell, we estimated the fraction of atoms with the local environment corresponding to the bcc lattice, i.e., the crystalline phase in the total number of simulated particles. The results of the calculation are shown in Fig. 5.

According to Fig. 5, the fraction of particles belonging to the crystalline phase gradually increases during the simulation, but, at the same time, an increase in the strain value reduces their fraction in the total number of particles, i.e., the crystallization front moves at a lower speed. This result was also confirmed by the visual observation of the computational cell. The flatter shape of the curves at the end of the simulation is due to the fact that crystallization is completed and the remaining particles, which are not identified as a bcc crystal, belong to the surface layer (see Fig. 3c). It should be noted that, under tension, despite a decrease in the speed of the crystallization front at the beginning of the simulation, the complete crystallization is still observed at the end. Apparently, in this case, the effect of reducing the activation energy of self-diffusion of atoms due to an increase in the free volume in the lattice is additionally manifested, which simplifies the crystallization.

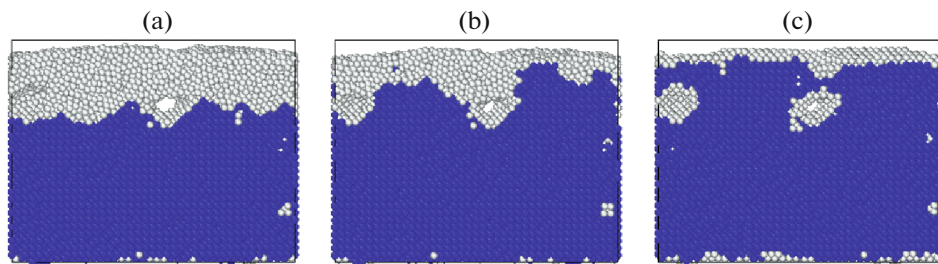


**Fig. 3.** Visualization of the computational cell upon annealing at a temperature of  $0.3T_{melt}$  after (a) 15, (b) 30, and (c) 60 ps.

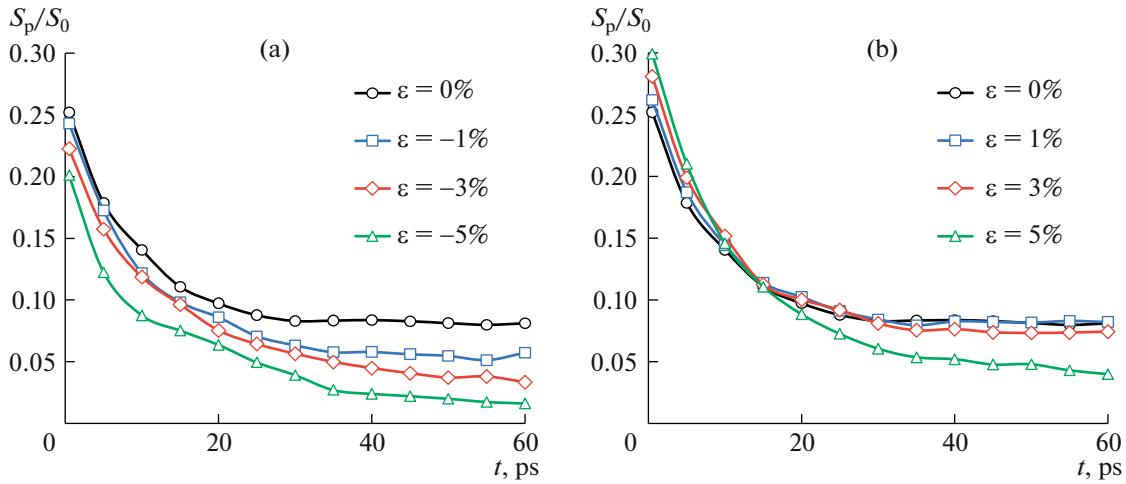


**Fig. 4.** Change in the relative free surface of pores in the computational cell during the simulation at different values of (a) the compressive and (b) tensile strain (the computational cell temperature is  $0.3T_{\text{melt}}$ ).

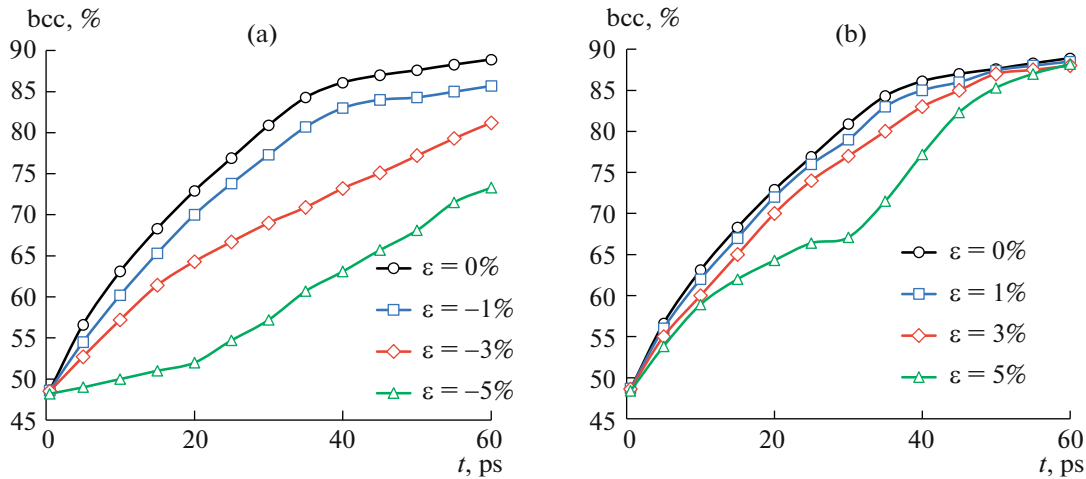


**Fig. 5.** Change in the fraction of particles in the computational cell the local environment of which corresponds to the bcc lattice during the simulation at different (a) compressive and (b) tensile strains (the computational cell temperature is  $0.3T_{\text{melt}}$ ).

## CONCLUSIONS

In this study, the results of the molecular dynamics simulation of the reduction of the volume of pores in the crystal that arose upon nonuniform heating of the computational cell as a result of the crystallization were presented. The main mechanism of the reduction is called the diffusion-viscous flow of matter into pores. Taking into account that, in the amorphous phase of a substance, the diffusion process proceeds more intensively than in the crystalline phase, a possible way to reduce the porosity of the surface layer of a material exposed to laser pulses can be its straining, which helps to reduce the speed of propagation of the crystallization front.

## FUNDING

This study was carried out within the State assignment no. 0809-2021-0013.

## CONFLICT OF INTEREST

The authors declare that they have no conflicts of interest.

## REFERENCES

1. E. B. Yakovlev, V. V. Svirina, and O. N. Sergaeva, *Izv. Vyssh. Uchebn. Zaved., Priborostr.* **53** (4), 57 (2010).
2. P. M. Kuznetsov and V. A. Fedorov, *Vestn. TGU* **15**, 1790 (2010).

3. N. A. Smirnov, S. I. Kudryashov, A. A. Rudenko, A. A. Nastulyavichus, and A. A. Ionin, *Laser Phys. Lett.* **19**, 026001 (2022).
4. S. V. Filaretov, E. A. Kashtanova, E. G. Zubkov, and A. A. Polyakov, *Izv. Vyssh. Uchebn. Zaved., Povolzh. Reg., Fiz.-Mat. Nauki*, No. 3 (27), 212 (2013).
5. B. Zhang, Y. Li, and Q. Bai, *Chin. J. Mech. Eng.* **30**, 515 (2017).
6. S. P. Murzin, A. B. Prokofiev, and A. I. Safin, *Proc. Eng.* **176**, 552 (2017).
7. A. N. Glotov, Yu. V. Golubenko, V. A. Desyatskov, and A. V. Stepanov, *Vestn. MGTU im. N. E. Baumana, Ser. Priborostr.*, No. 1, 15 (2020).
8. A. V. Markidonov, M. D. Starostenkov, A. N. Gostevskaya, D. A. Lubyanoi, and P. V. Zakharov, *Metall-oved. Term. Obrab. Met.*, No. 5 (803), 16 (2022).
9. A. V. Markidonov, A. N. Gostevskaya, V. E. Gromov, M. D. Starostenkov, and P. A. Zykov, *Deform. Razrush. Mater.*, No. 8, 2 (2022).
10. M. I. Mendeleev, S. Han, D. J. Srolovitz, G. J. Ackland, D. Y. Sun, and M. Asta, *Philos. Mag.* **83**, 3977 (2003).
11. XMD—Molecular Dynamics Program. <https://xmd.sourceforge.net>. Accessed April 11, 2023.
12. G. J. Ackland and A. P. Jones, *Phys. Rev. B* **73**, 054104 (2006).
13. OVITO—Open Visualization Tool. <https://www.ovito.org>. Accessed April 11, 2023.
14. A. I. Mikhailin and I. A. Slutsker, *Sov. Tech. Phys. Lett.* **17**, 539 (1991).
15. D. K. Belashchenko, *Phys. Usp.* **42**, 297 (1999).

*Translated by E. Bondareva*